

Electrochemical Impedance Spectroscopy Study of the Adsorption Behavior of Bovine Serum Albumin at Biomimetic Calcium – Phosphate Coating

Q. Mohsen¹, Sahar A. Fadl-allah^{1, 2, *} and Nahla S. El-Shenawy^{3, 4}

¹ Materials and Corrosion Lab (MCL), Faculty of Science, Taif University, Taif, K.S.A

² Chemistry Department, Faculty of Science, Cairo University, Giza, Egypt

³ Zoology Department, Faculty of Science, Taif University, Taif, K.S.A

⁴ Zoology Department, Faculty of Science, Suez Canal University, Ismailia, Egypt

*E-mail: Sahar.fadlallah@yahoo.com

Received: 22 March 2012 / Accepted: 12 April 2012 / Published: 1 May 2012

The electrochemical impedance spectroscopy, EIS, was used to investigate the interfacial behavior of bovine serum albumin (BSA) on different titanium (Ti) surfaces at open circuit potential. Nano porous titanium oxide film, TiO₂, was anodically formed on titanium from electrolyte containing 1M H₂SO₄ and 0.5% wt NaF at 20 V for 20 min. The biomimetic calcium-phosphate coating was deposited cathodically on anodized titanium, (AT) from supersaturated calcium-phosphate solution, SCPS, at low temperature, 60°C. To be the Ti, AT, and Ca-P/AT surfaces have been used to compare among microstructures and protein adsorption behavior. Island from calcium–phosphate coating was detected by the scanning electron microscope, SEM. The electron diffraction X-ray analysis, EDX, was used to investigate the difference in chemical structures between different types of examined surfaces. The experimental impedance data were fitted to theoretical data according to proposed equivalent circuit models. The impedance data fitting enabled to explain the adsorption phenomena of BSA occurred on the different specimen's surface. This work indicated formation of nano-TiO₂ film on Ti improved the Ca-P induction ability which enhanced the adsorption of BSA on its surface.

Keywords: Titania, Thin film, Electrochemical Impedance Spectroscopy, Scanning Electron Microscope, Albumin Adsorption, Biomimetic Ca-P coat.

1. INTRODUCTION

For last decade, titanium (Ti) and titanium alloys has emerge as a magic metal for bone replacement due to their biocompatibility, excellent corrosion resistance, and sufficiently strong for use as load-bearing and machinable orthopedic implant materials. For these reasons, they have been

used successfully as orthopedic and dental implants [1]. Ti without any surface treatment is bioinert, not bioactive. To further improve the bioactivity and biocompatibility of Ti, various types of surface modification method have been explored. Our Previous research has shown that it is possible to increase the range of biomaterials application by depositing a thicker layer of titanium oxide, TiO_2 on the metal surface [2, 3].

Various coatings have been attempted to provide Ti and its alloys with bond-bonding ability, which spontaneously bond to living bone [4]. Recently, biomimetic methods to produce calcium-phosphate (Ca-P) coatings have attracted considerable research attention [5-8]. The biomimetic methods produce Ca-P coatings by immersing metal implants in aqueous solution containing calcium and phosphate ions at certain physiological temperature and pH. Various techniques have been developed to deposit bioactive Ca-P coating on Ti substrate, such as plasma spraying [9, 10], sol-gel deposition [11], sputtering [12], pulsed laser application [13], electrochemical deposition [14], biomimetic method [15], and anodization [16, 17].

Biomimetic coating requires pretreatment of Ti surface because untreated Ti surfaces cannot induce Ca-P nucleation in simulated physiological environments or in supersaturated aqueous solutions. Several methods to treat Ti surfaces to give them Ca-P induction ability have been introduced [18, 19]. A more recent method is micro arc anodic oxidation, which can produce a micro porous layer of anatase on the surface of Ti metal, there by accelerating the Ca-P inducing ability in simulated body fluid [20-22].

Protein adsorption is an initial event that occurs when biomaterials come into intimate contact with the body, and it's the nature of this protein-surface interaction that apparently governs the cellular responses that follow. The types, orientations and conformations of protein adsorbed to a surface are extremely important. Protein must bind to a surface "properly" in order to make natural body response [23].

The interaction between proteins and surfaces has been found to be sensitive to surface characteristics of the metals on to which adsorption occurs. Therefore, many studies leading to a better fundamental understanding of the properties and mechanisms that govern protein adsorption are particularly important for many disciplines.

The adsorption behavior of albumin which it considers one of the main constituents of blood was investigated [24, 25]. Byrne et al [26] found that there are a wide variety of techniques that have been used to investigate protein adsorption as ellipsometry [26, 27], atomic force microscopy (AFM) [28], X-ray photoelectron spectroscopy (XPS) [29] and tracking of fluorescent of radioactively tagged proteins [30]. They aimed to understand the influence of albumin in the change of the characteristics of passive films to be suitable for implantation in human bodies, especially in bone surgeries and dental implants.

The present study was concerned on three objectives: (i) synthesis of nano TiO_2 oxide film produced by anodic oxidation from acidic NaF solution, (ii) induct biomimetic Ca-P coat on the TiO_2 film and (iii) estimate the albumin adsorption behavior of different studied titanium surfaces by using electrochemical impedance spectroscopy.

2. EXPERIMENTAL

2.1 Materials and Solutions

Titanium foil (SIGMA-ALDRICH CHEMIE GmbH, Riedstr.2D-89555 Steinheim 49 7329 970) with 0.25 mm thick, 99.7% metals basis was used as a base material in this study. All specimens were cold mounted with epoxy resin. The exposed metal surface (area: 1cm^2) of each specimen was ground with silicon carbide paper to 2000 grit, washed in distilled water and then rinsed with alcohol before corrosion test. The surface obtained by the mechanical polishing process was studied and it is denominated by Ti sample.

The supersaturated calcium- phosphate solution, SCPS, was used as an example for physiological solution. SCPS was prepared by dissolving NaCl (7.714 g), CaCl_2 (1.387 g), $\text{Na}_2\text{HPO}_4 \cdot 2\text{H}_2\text{O}$ (0.89 g) and 1 M HCl 50 ml in one liter of deionized water. Tris-hydroxymethyl amino methane (TRIS) was used to adjust the pH value to 6.2 in order to maintain the chemical stability of the solution. Bovine serum albumin, BSA, was dissolved in SCPS solution at a concentration of 2 mg/liter at 37°C .

2.2 Anodic oxidation treatment

The electrolyte used in this work to anodize Ti is contained 1M H_2SO_4 and 0.5 % wt NaF to obtain nano- TiO_2 film by using a two-electrode cell. Rectangular samples of titanium area 1cm^2 were used as the anode and a platinum plate of area $3 \times 3\text{cm}^2$ was used as the cathode. The anodization treatment was occurred in the following sequence: (a) mechanical polishing, (b) The metallic sheet was then cleaned ultrasonically in acetone and (c) anodizing at 20 V in the electrolytic bath for 20 min. The surface obtained by the method previously described was studied and it is denominated by the AT sample.

2.3 Electrodeposition of biomimetic Ca-P coat

The biomimetic Ca-P coat was electrodeposited on the AT surface. Electrodeposition was carried out in a standard two-electrode cell in which AT was used as a cathode and a platinum plate of area $3 \times 3\text{cm}^2$ was used as the anode. This coat was deposited cathodically at 2V for an hour in supersaturated calcium-phosphate solution, SCPS, what was heated at low temperature 60°C . The solution was adjusted at pH of 7.4 with tri-hydroxymethylaminomethane $[(\text{CH}_2\text{OH})_3\text{CNH}_2]$ and hydrochloric acid. The surface obtained by the method previously described was studied and it is denominated by the Ca-P/AT sample.

2.4 Electrochemical impedance spectroscopy, EIS, measurements

The electrochemical behavior of the different titanium samples (Ti, AT, Ca-P/AT) in SCPS at 37°C solution as a function of the immersion time was studied by electrochemical impedance

spectroscopy, EIS. EIS is a non-destructive sensitive technique which enables the detection of any changes occurring at the electrode /electrolyte interface.

All electrochemical experiments and EIS measurements were carried out using a potentiostat AUTOLAB model PGSTAT 30 with FRA modules. In a one compartment three-electrode cell where Ti or AT or Ca-P/AT electrodes as working electrodes, platinum coiled wire as a counter electrode, and a saturated calomel electrode, SCE, as a reference electrode were used, respectively. All EIS spectra were obtained by applying the open circuit potential at a frequency range of 10^{-1} – 10^5 Hz to evaluate the structure stability of different titanium surface in SCPS. The impedance spectra are displayed as a Bode diagrams (impedance modulus and phase angle vs. frequency) and Nyquist diagrams (Real impedance vs. imaginary impedance). From Bode & Nyquist plots, equivalent circuits that fit the experimental data were proposed. EIS results were interpreted using a fitting procedure fit program FRA [2,3] and based on equivalent circuit model presented on Fig.1.

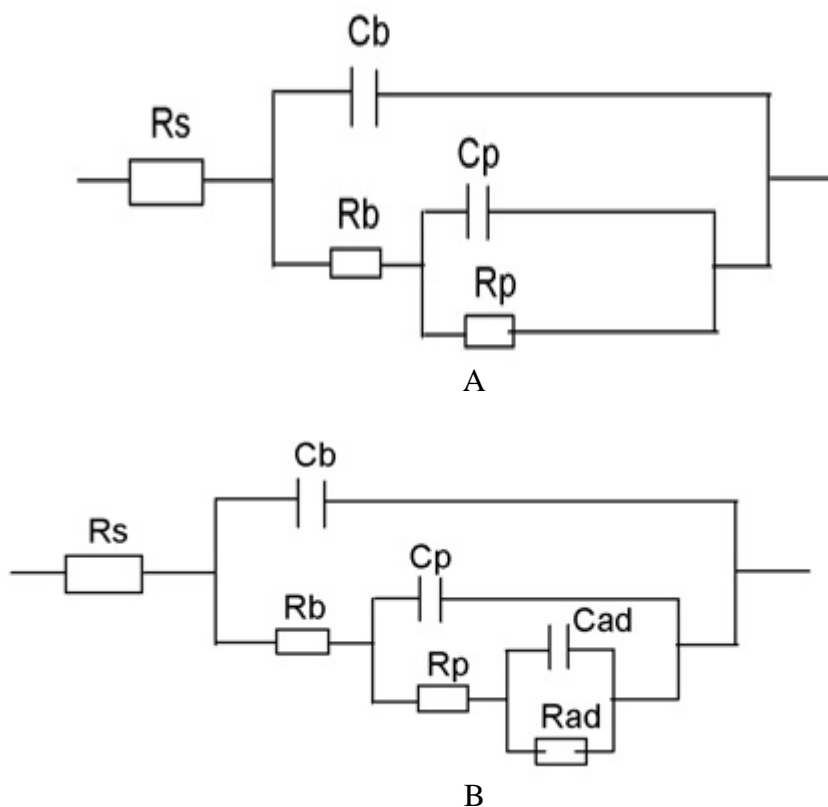


Figure 1. (a) Literature equivalent circuit (b) Modified equivalent circuit used for fitting experimental impedance data.

Constant phase element, CPE, was introduced instead of pure capacitors in the fitting procedure to obtain good agreement between the simulated and experimental data. The impedance of CPE is defined as $Z_{CPE} = 1/(Q(j\omega)^n)$, where $Q(\omega^{-1} s^n cm^{-2})$ is the combination of properties related to both the surface and the electro active species independent on frequency, “n” is related to a slope of the $\log Z$ vs. $\log f$ and ω is the angular frequency.

2.5 Morphology characterization and chemical composition of samples

The surface morphology and chemical composition of the different titanium samples (Ti, AT and Ca-P/AT) were studied by scanning electron microscope (SEM) electron diffraction X-ray (EDX) and analysis by JEOL-840 electron prop micro analyzer.

3. RESULTS AND DISCUSSION

3.1 Characterization of samples surface

3.1.1 Ti sample

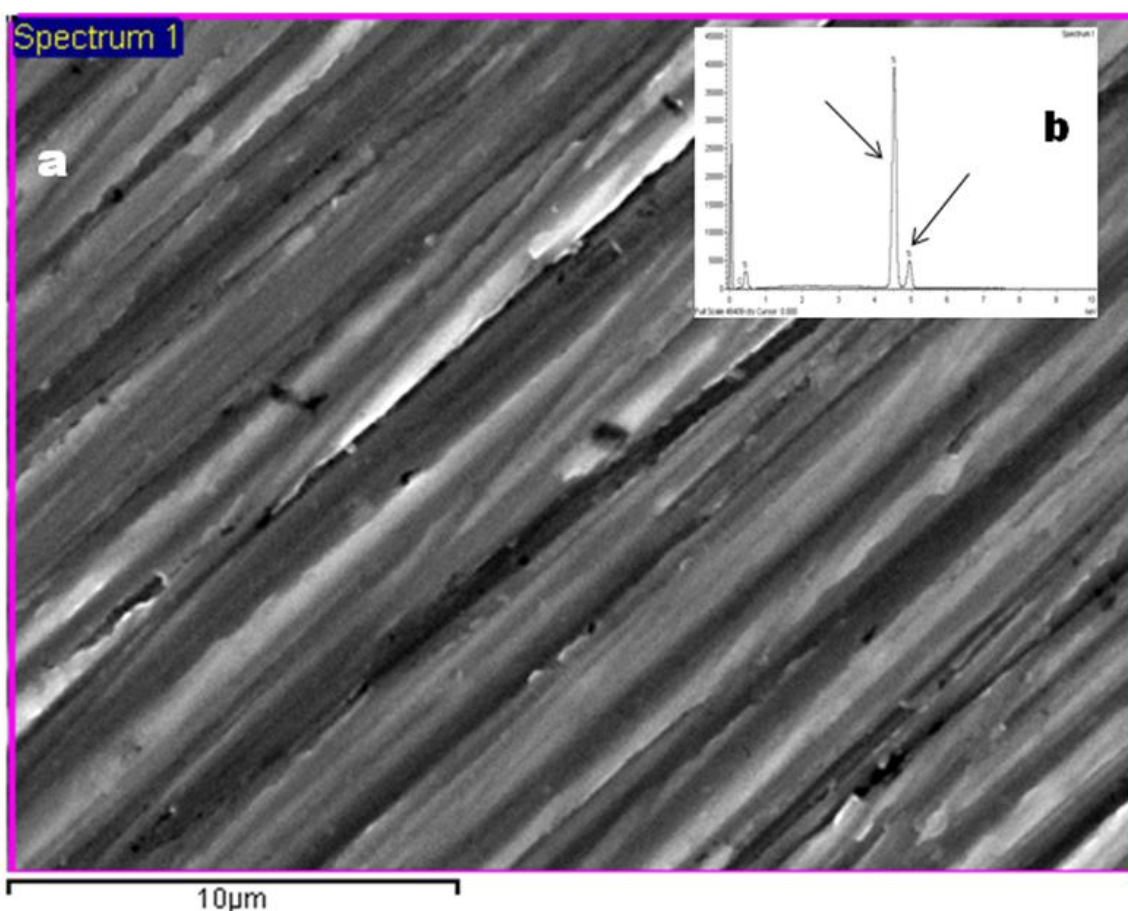


Figure 2. (a) SE micrographs showing the surface morphology of Ti sample, magnification 1000x (b) EDX patterns of Ti sample.

To study the morphology and structure of the untreated titanium sample (Ti), SEM and EDX investigations were carried out. Fig. 2a shows the surface appearance of the mechanically polished Ti represented the typical morphology of the native oxide film with thin, non-porous structure, amorphous and good adherent [2]. This oxide film is spontaneously formed on the Ti surface on

exposure to air at room temperature [3]. The major chemical element is Ti which supported through EDX analysis (Fig. 2b). The results of the EDX analysis were presented in Table 1.

Table 1. Chemical Composition wt% of different titanium samples

Samples	O	Na	P	Ca	Ti	Total
Ti	-	-	-	-	100	100
AT	21.78	-	-	-	77.94	
Ca-P/AT	43.79	0.58	7.65	10.86	37.22	100

3.1.2 AT sample

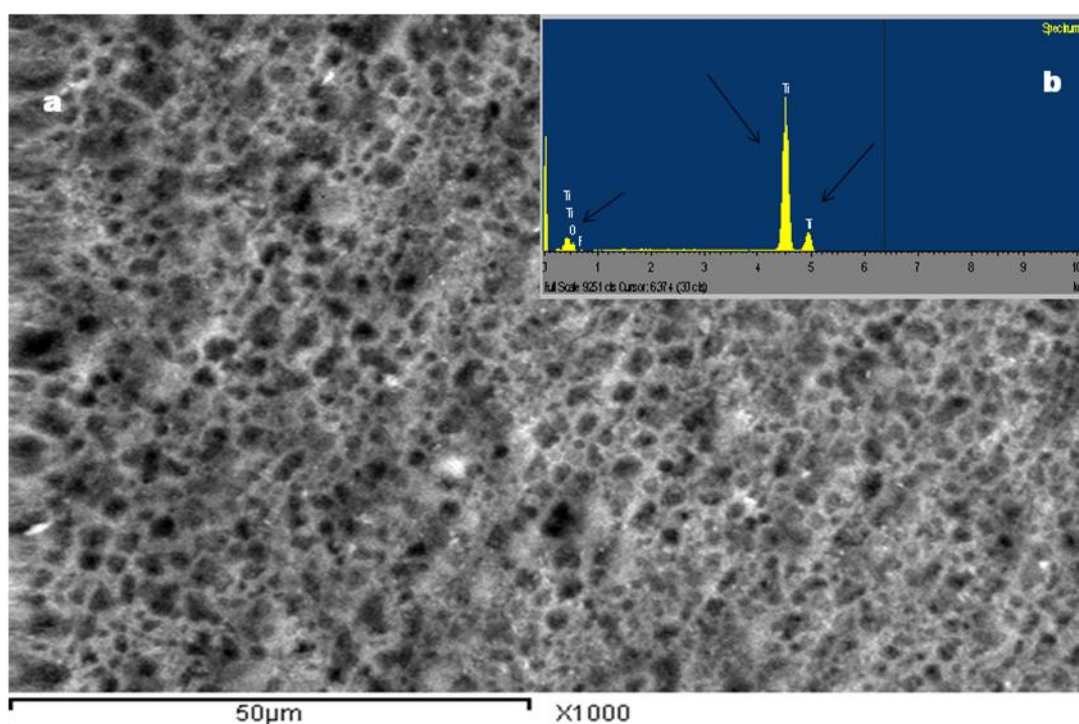


Figure 3. (a) SE micrograph of TiO_2 formed by anodic oxidation of titanium the surface in $1\text{M H}_2\text{SO}_4 + 0.5\text{ wt\% NaF}$ for 20 min at 20 V, TiO_2/Ti sample, magnification 1000x (b) EDX survey of TiO_2 formed by anodic oxidation of titanium in $1\text{M H}_2\text{SO}_4 + 0.5\text{ wt\%}$ for 20 min at 20 V, TiO_2/Ti sample.

Side with SEM and EDX investigations, we were able to explore the morphology and chemical composition of AT sample. Fig. 3a shows that the oxide film of the network forms with nano porous slots. Fig. 3b represented the EDX scan spectra of the AT electrode. Fig. 3b and Table 1 indicated that the chemical composition of the oxide layer is Ti and oxygen. Without any doubt that the oxide film formed in $1\text{M H}_2\text{SO}_4$ and 0.5 Wt% NaF is more nano porous than that formed in our previous work [3, 31]. Nano TiO_2 can be prepared by various techniques such as sol-gel method [32], electrophoretic deposition method [33] and anodization method [34]. Anodization is extremely preferred, because it

provides strongly adherent TiO_2 layer than the other two methods. So it accepted that this type of oxide film treatment is more benefit and capable of incorporating Ca and P from the physiological solution.

3.1.3 Biomimetic Ca-P/ TiO_2 /Ti sample

In the present study, the method of Ca-P deposition was developed. A thick and crystallized Ca-P coating was easily electrochemically deposited on the AT surface from supersaturated Ca-P solution at low temperature.

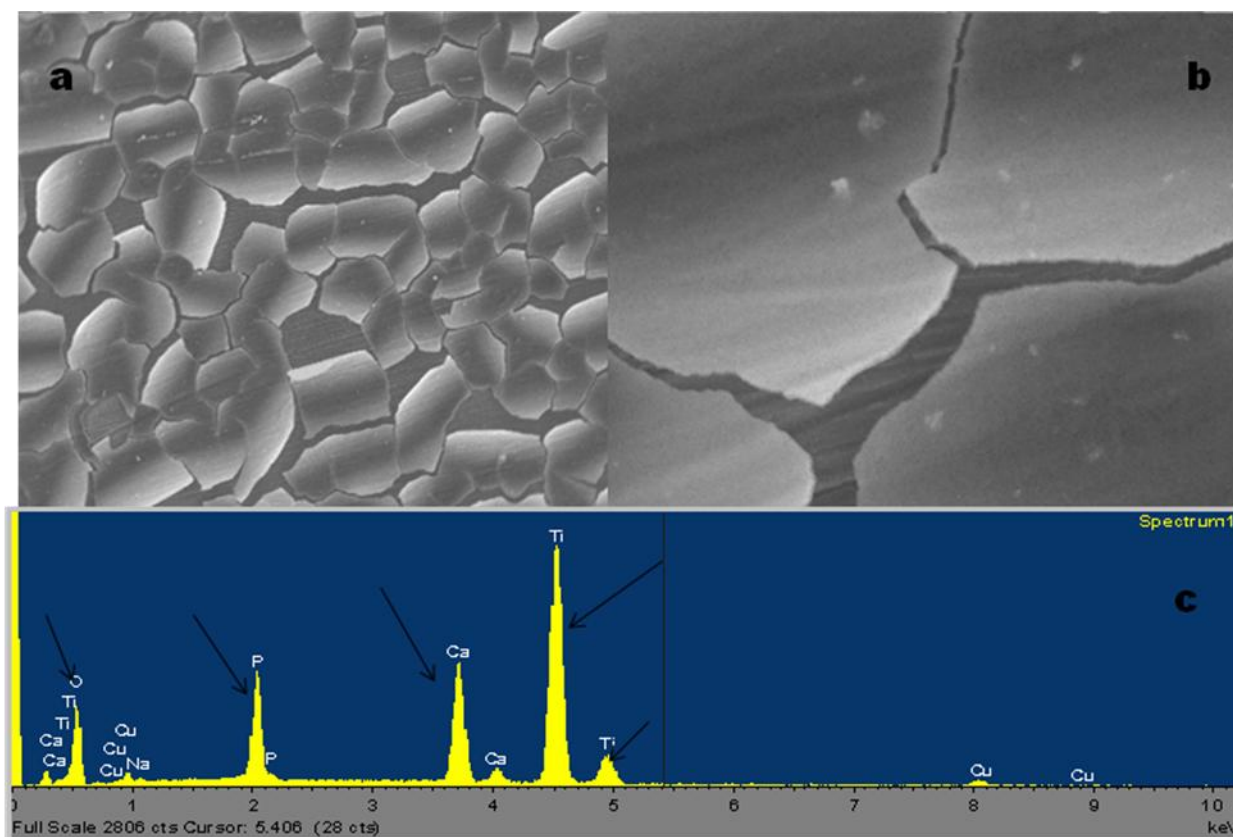


Figure 4. (a) SE micrograph of Ca-P layer formed by cathodic deposition of TiO_2/Ti in SCPS at pH 7.4, 60°C , and constant potential of 2V for 1h, Ca-P/ TiO_2/Ti sample ,magnification 1000x (b) SE micrograph of Ca-P layer formed by cathodic deposition of TiO_2/Ti in SCPS at pH 7.4, 60°C , and constant potential of 2V for 1h, Ca-P/ TiO_2/Ti sample ,magnification 5000x (c) EDX survey of Ca-P layer formed by cathodic deposition of TiO_2/Ti in SCPS at pH 7.4, 60°C , and constant potential of 2V for 1h, Ca-P/ TiO_2/Ti sample.

The SEM (Figs. 4a, 4b) and EDX (Fig.4c) analysis of Ca-P/AT surface were investigated. The surface of AT sample was covered with plate-like crystals from Ca-P with regular shape. SEM of biomimetic Ca-P coat by two different magnification, Fig.4a and 4b show a good adhesion between the Ca-P coat and the AT surface. The present results refer to the deposition of Ca and P on AT surface is more benefit than the deposition on the polished Ti that has been previously studied [35]. The signal of

Ca and P (Fig.4c) confirmed the present of these elements in Ca-P coat. Ca/P ratio in the present coating is equivalent to the natural hydroxyapatite ratio (Table 1). This result is in agreement with the pervious study [15]. They form the same uniform layer of Ca-P but under strong treatment condition and after long immersion in simulated buffer solution.

3.2 Electrochemical measurements

3.2.1 OPC measurements

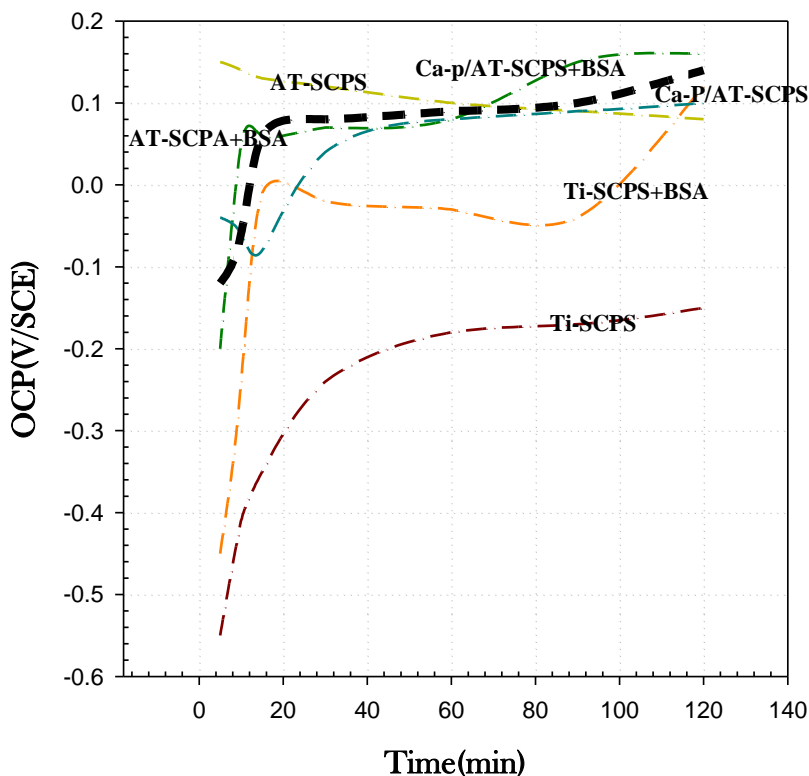


Figure 5. Variation of OCP with time for Ti sample, anodized specimen TiO_2/Ti sample, and Ca-P/ TiO_2/Ti sample exposed to SCPS solution at 37°C .

Fig. 5 illustrated the variation of open circuit potential (OCP) with time for different titanium samples (Ti, AT and Ca-P/AT) in SCPS solution with and without BSA at 37°C . The data of the initial OCP illustrated the role of BSA on the different surfaces in the supersaturated calcium–phosphate solution (Table 2). From these results, we could prove that the untreated Ti surface is unstable in the simulated biological solution which containing or non-containing BSA. Generally, the OCP of Ti sample was found to be shifted towards the positive potential region after three hours of immersion in SCPS with BSA. On the other side the AT and the biomimetic Ca-P/AT samples represented the good way to increase the life of the Ti metal in physiological solution, because they demonstrated a similar trend of variation in the examined solution. 20 min needed to attain the steady state values of OCP. This time decreased to about 5-10 min by addition of BSA.

Table 2. Values of OCP of different titanium samples in SCPS solution with and without BSA at 37°C

Metal Surface	SCPS without BSA		SCPS with BSA	
	Initial OCP (mV (SCE))	OCP after 2h (mV (SCE))	Initial OCP (mV (SCE))	OCP after 2h (mV (SCE))
Ti	-530	-140	-445	120
AT	145	120	-200	160
Ca-P/AT	-40	100	-120	140

This result refers to the homogeneity of these samples in the physiological solution. To ensure complete characterization of the electrode / electrolyte interface and processes that occur on samples surface, EIS measurements were made in a wide frequency range after stabilization of the different testing electrodes for 30 min at the OCP. The EIS spectra recorded in absence and in presence of BSA in SCPS.

3.2.2 EIS of Ti sample

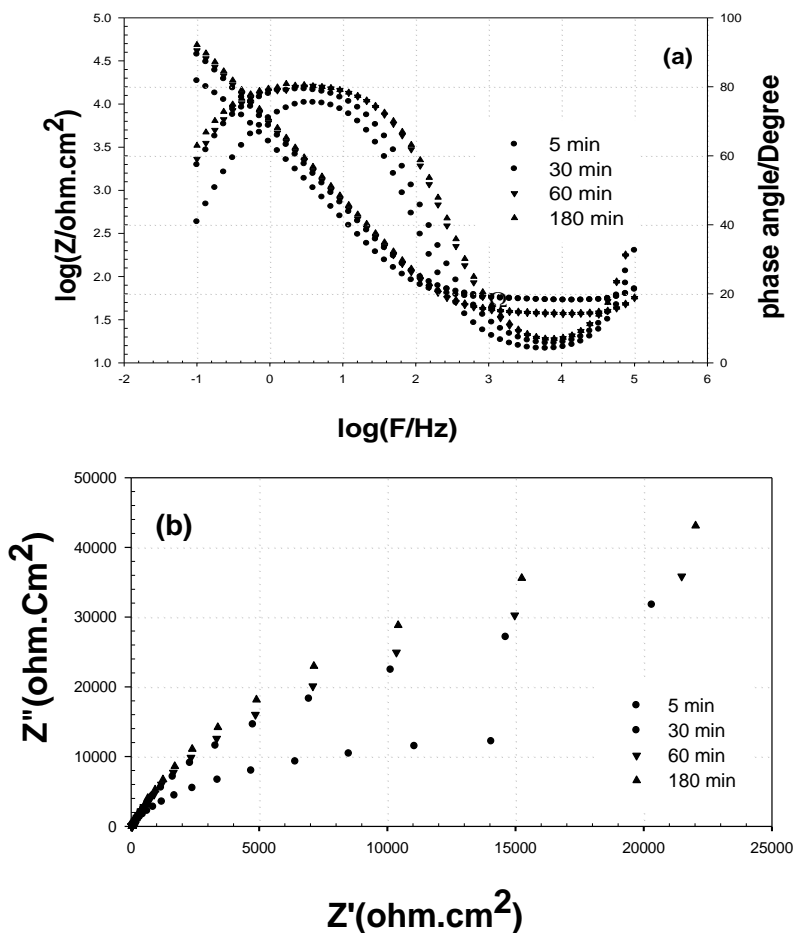


Figure 6. Impedance data recorded on Ti sample for different time of immersion at 37°C in SCPS without Bovine Serum Albumin BSA (a) Bode plot (b) Nyquist plot.

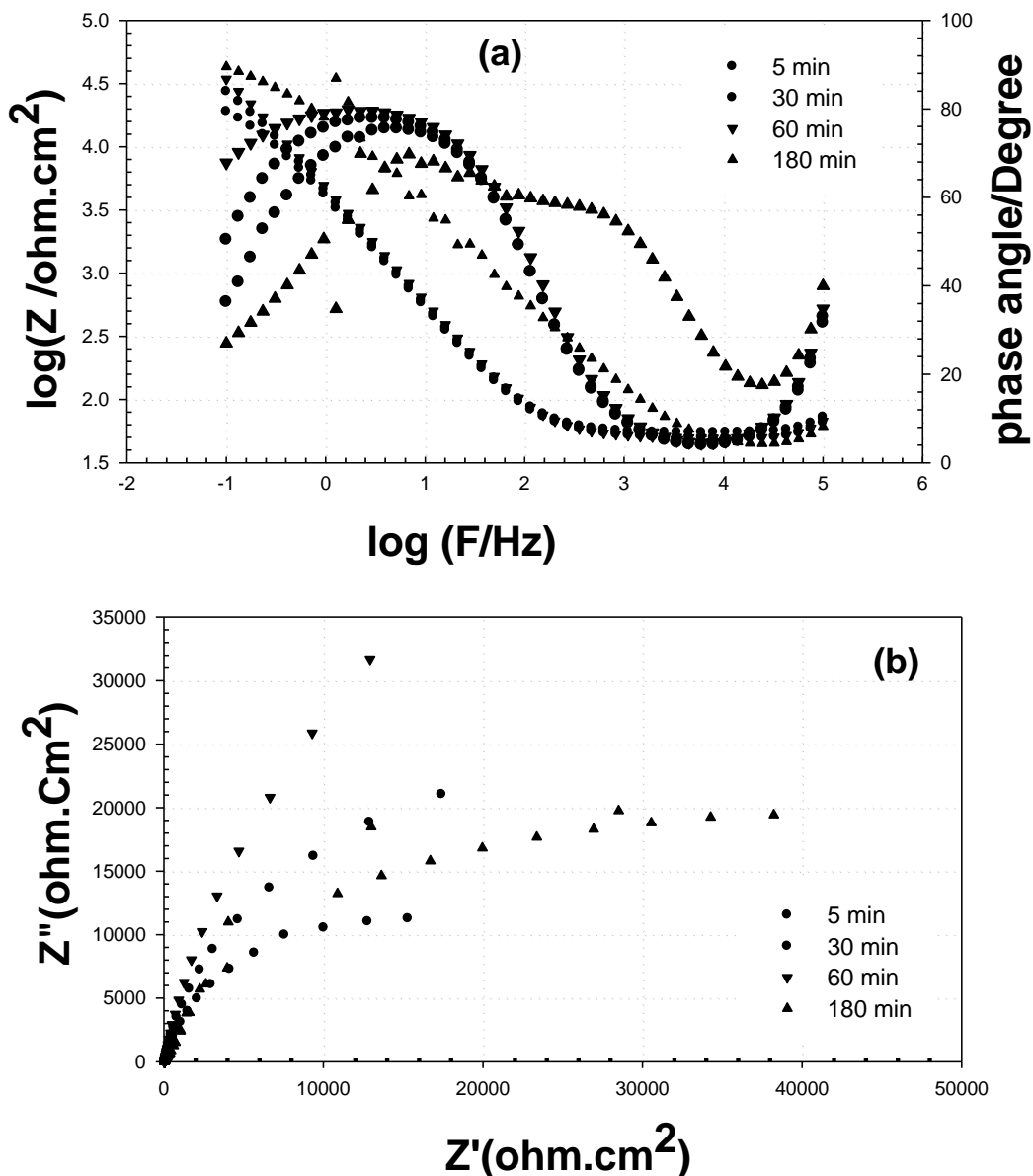


Figure 7. Impedance data recorded on Ti sample for different time of immersion at 37°C in SCPS with Bovine Serum Albumin BSA (a) Bode plot (b) Nyquist plot.

The results of EIS tests are presented through Bode and Nyquist diagrams. These diagrams for the Ti surface after 3 hrs immersion in SCPS solution at 37°C in absence or in presence of BSA are shown in Figs. 6 and 7, respectively. When Ti is exposed to SCPS solution without any addition of BSA, its EIS spectra exhibit behavior typical of a thin passive oxide film on Ti, i.e., a near – capacitive response illustrated by a phase angle close to -90° over a wide frequency range. Furthermore, these data were changed with exposure time (Fig. 6a), indicates that the Ti sample became more stable with the time of immersion in SCPS without BSA. Nyquist plot shows the impedance increases with time of immersion (Fig.6b).

However, when Ti is exposed to SCPS with an addition of BSA, the spectrum appears different and varies significantly with exposure time. A set of spectra at different exposure times is shown in

Fig.7. Clear from Fig. 7a, the impedance changed with time of immersion especially at the intermediate frequency region. After three hours of immersion, the two maxima appear clear with a lower in phase angle.

The results show that the untreated Ti surface decrease albumin adsorption and support the behavior of BSA which can enhance the dissolution of the passive oxide film on the surface, thus may increase the corrosion of the metal [36, 37]. Nyquist plot supports also the same behavior of Ti sample in SCPS with BSA, Fig.7b. This result confirmed that Ti which is used in the majority of implants needs to be developed to operate effectively in a biological environment [25].

3.2.3 EIS of AT sample

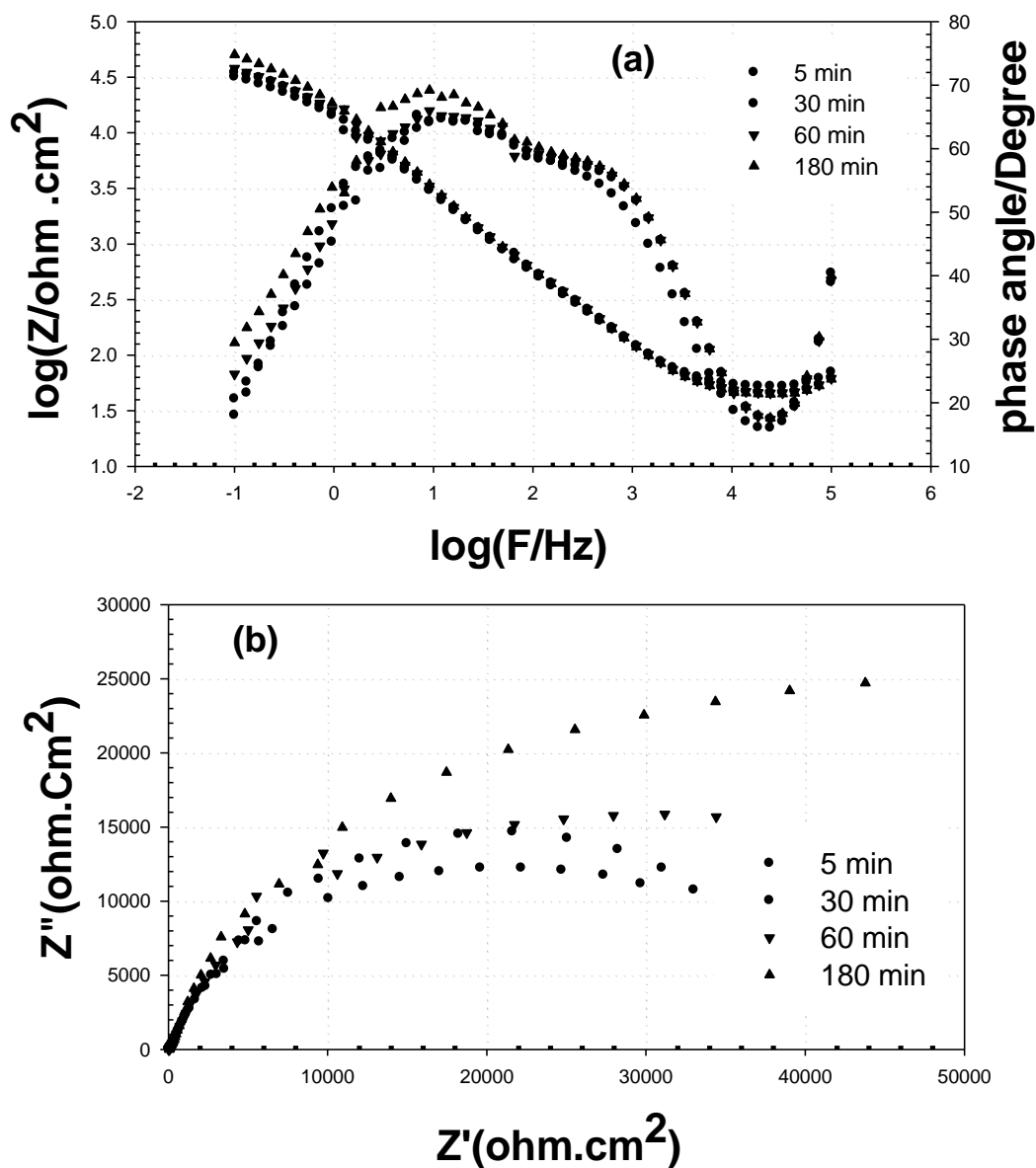


Figure 8. Impedance data recorded on TiO₂/Ti sample for different time of immersion at 37°C in SCPS without Bovine Serum Albumin BSA (a) Bode plot (b) Nyquist plot.

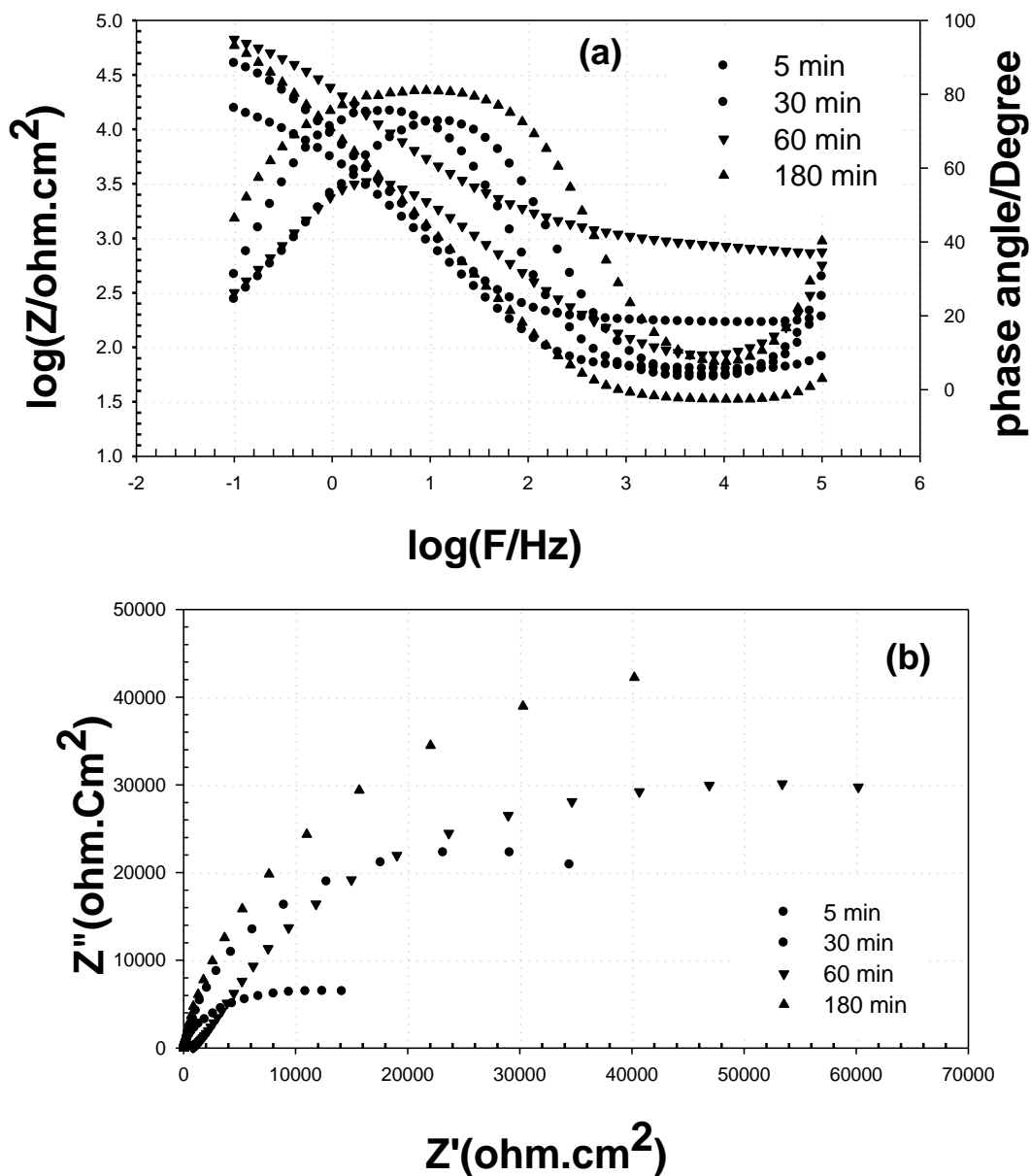


Figure 9. Impedance data recorded on TiO_2/Ti sample for different time of immersion at 37°C in SCPS with Bovine Serum Albumin BSA (a) Bode plot (b) Nyquist plot.

The morphology of AT surface which appears as nano porous layer was presented in Fig.3a. The EIS diagrams for this AT surface after 3 hrs in SCPS solution at 37°C in absence or in presence of BSA are shown in Figs. 8 and 9, respectively. These figures showed that the change of surface from untreated Ti to oxide AT surface play an important role to change the behavior of the oxide surface in the SCPS solution in absence or in presence of BSA. In the solution without BSA, two relaxation time constants were clearly indicated by two peaks on phase angle plot (Fig. 8a). This indicates and confirms that the oxide film formed on Ti by the solution as mentioned in the experimental section is composed of a porous outer layer and a barrier inner layer [38]. It is clear that the impedance increases with time from the Nyquist plot (Fig.8b). This explain that the nano porous layer of TiO_2 allow the

entry of ions from the physiological solution and filled the pores in the outer porous layer which increases the stability of passive film. This refer to the increased surface area of the TiO_2 is useful for accelerated bone growth in orthopedic / dental applications [39].

EIS spectra in presence of BSA illustrate that BSA played a negative role in the first hour of immersion in SCPS. However, extending the experiment for three hours showed the positive roles of protein which increase the impedance especially in the low frequency region (Fig. 9a). BSA also integrate the two phase peaks and increase the capacitive response by a phase angle close to -90° over a wide frequency range. These results indicated that TiO_2 film is also stable in presence of BSA and confirm that the adsorption of proteins is clearly spontaneous [24]. The increase of impedance with the time of immersion is very clear in the Nyquist plot (Fig. 9b). These results support two main ideas that albumin is most readily adsorbed on the oxidized surface and it's adsorption to a surface is a good passivating process [25, 37].

3.2.4 EIS of Ca-P/AT sample

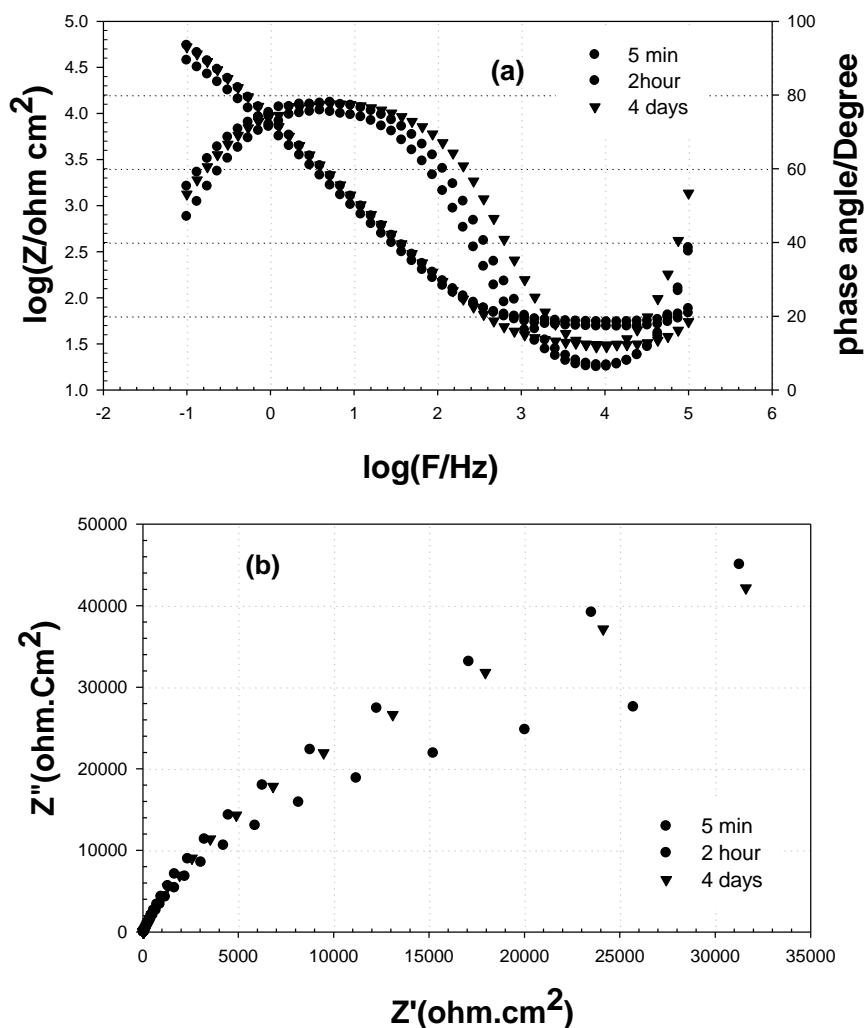


Figure 10. Impedance data recorded on Ca-P/ TiO_2 /Ti sample for different time of immersion at 37°C in SCPS without Bovine Serum Albumin BSA (a) Bode plot (b) Nyquist plot.

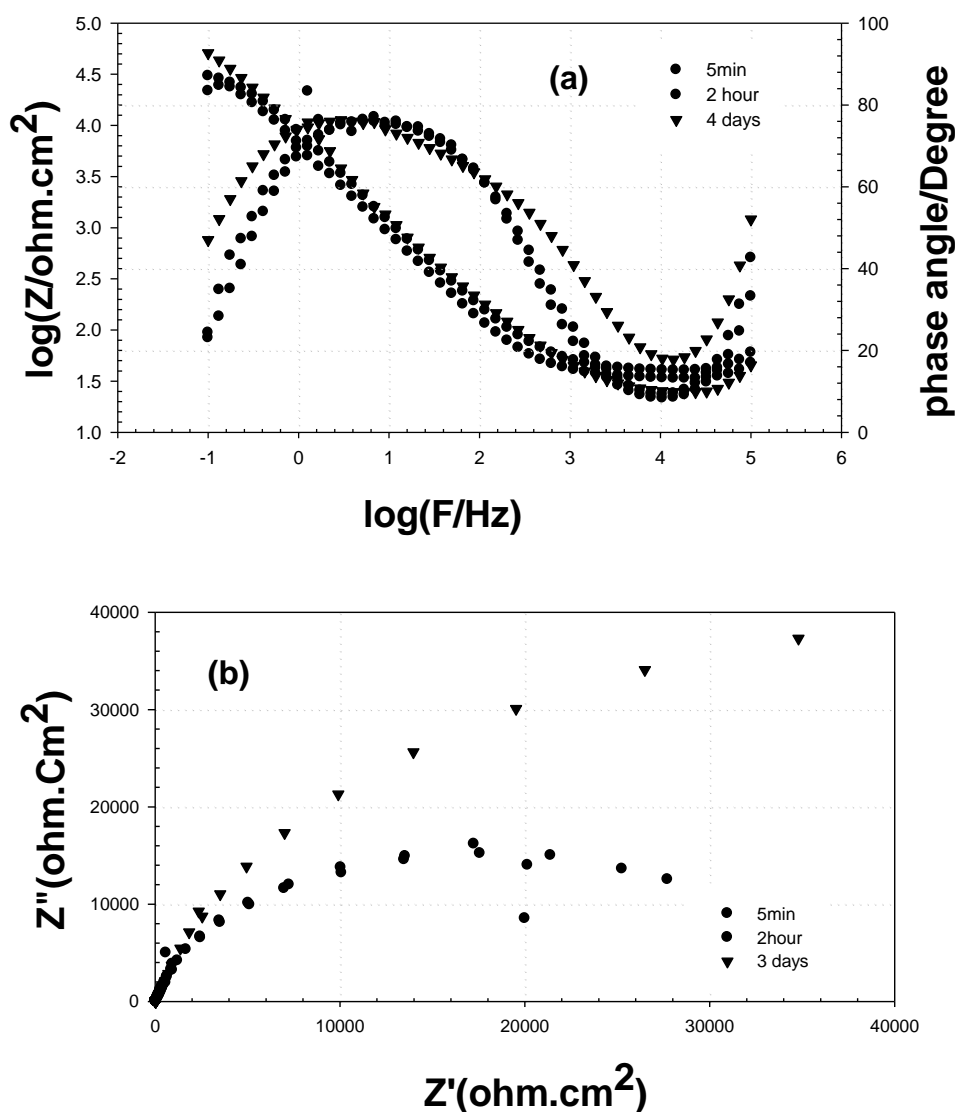
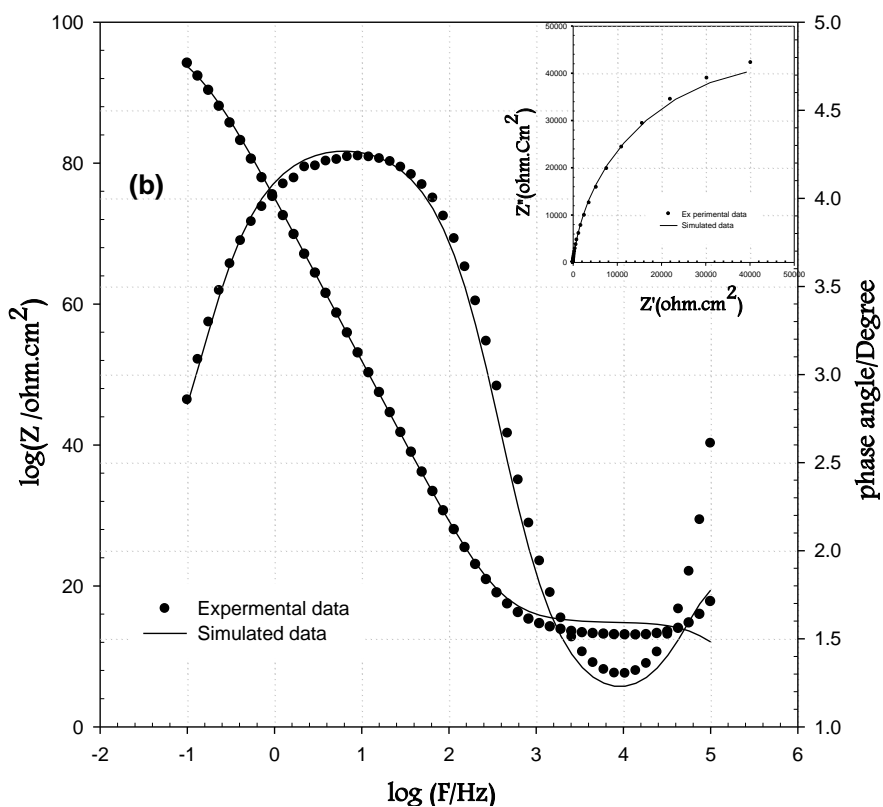
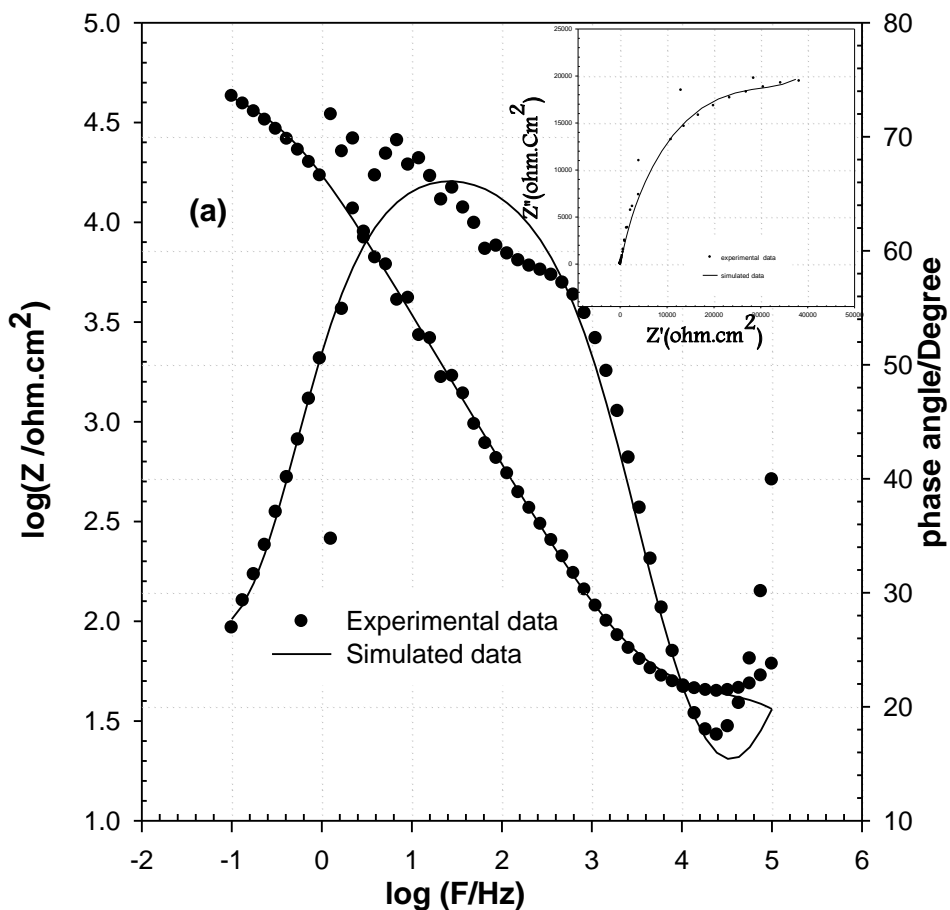


Figure 11. Impedance data recorded on Ca-P/TiO₂/Ti sample for different time of immersion at 37°C in SCPS with Bovine Serum Albumin BSA (a) Bode plot (b) Nyquist plot.

Figs. 10 and 11 showed electrochemical impedance data for Ca-P plates which presented in Fig.4a and formed on nano-porous AT samples in the form of Bode and Nyquist diagrams. These diagrams represent the Ca-P/AT surface after 4 days immersion, for more clarification on this new surface, in SCPS solution at 37°C in absence or in presence of BSA under open circuit potential. The general features of the bode impedance plots are consistent with passive film behavior which a phase angle approaching 90° over a wide range of frequency (Figs. 10a and 11a). No significant changes were recorded in impedance spectra either in absence or in presence of BSA. These results indicated that the Ca-P layer plays an important role to maintain the stability of Ti surface in a biological environment. The Nyquist plots, confirmed the results of bode plots (Figs.10b and 11b). These results are indicated that the TiO₂ nano-porous film is considered as an excellent base for biomimetic Ca-P layer and also in agreement with the observations of Narayanan et al. [40].

3.2.5 Fitting and interpretation



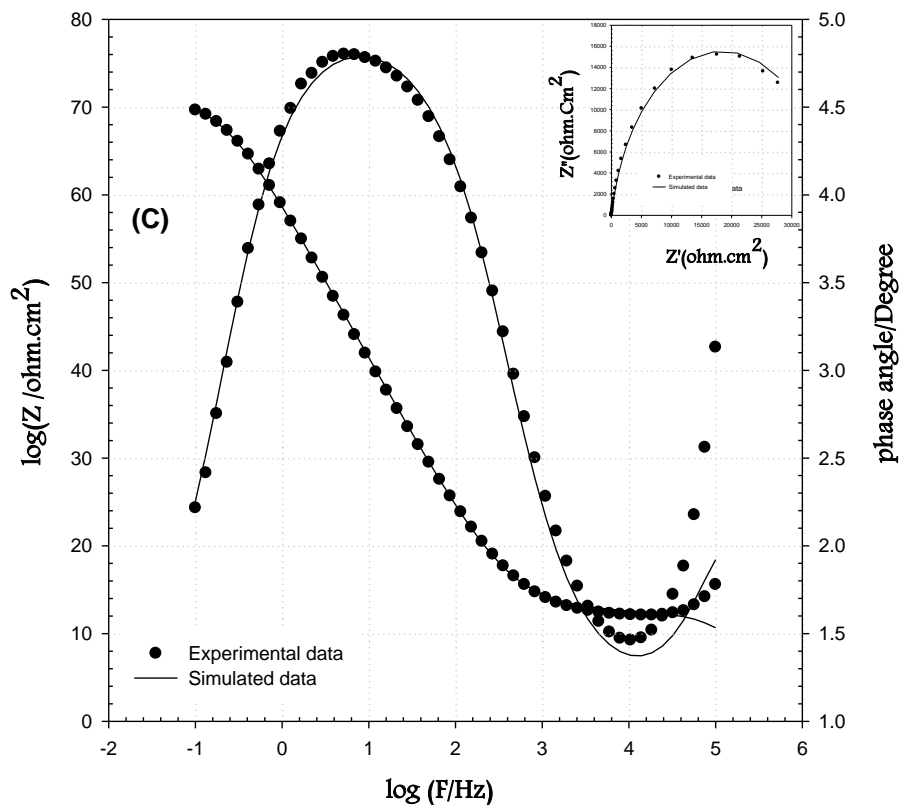


Figure 12. Comparing impedance data recorded on (a) Ti (b) TiO_2/Ti (c) $\text{Ca-P}/\text{TiO}_2/\text{Ti}$ after 3h of immersion at 37°C in SCPS with Bovine Serum Albumin BSA. Solid lines (—) represents simulated data.

Based on literature reports, equivalent electrical circuits have been used by many authors to interpret EIS results [41, 42]. Pan et al [42] was first use equivalent circuit presented in Fig. 1a to simulate data for Ti in saline solutions. This circuit can be regarded as an electrical representation of a two layer model of the oxide film consists of a barrier compact inner film and a porous outer layer. This model consists of a resistor, R_s , representing the solution resistance in series to two parallel combinations, R_b and C_b representing the resistance and capacitance of the inner barrier film and then R_p and C_p , representing the outer porous film resistance and capacitance, respectively. It was essential to modify the equivalent circuit presented in Fig.1a to obtain a better agreement between theoretical and experimental data for all impedance curves of AT and $\text{Ca-P}/\text{AT}$ in SCPS with BSA (Fig.12b and 12c), respectively. R-C combination was introduced to get the equivalent circuit (Fig.1b). This circuit account for the relatively thick adsorption layer formed on both electrode surfaces in the presence of BSA. Badawy et al [43] used this modified circuit to clarify the adsorption of Ca^{+2} on the Ti surface. The worst agreement between theoretical and experimental data is recorded for impedance curves of Ti in SCPS with BSA (Fig.12a). This result confirmed that the untreated Ti surface decrease albumin adsorption [37]. The pure capacitance present in the circuit (Fig.1b) is in fact constant phase elements (CPE) which usually are associated to rough and porous surfaces. CPE is given as both the parameters

Q and the exponent “ n ”. The exponent n is related to a slope of $\log Z$ against $\log f$ Bode plot. It should be stressed that for simplicity Q is often considered as a pure capacitance [24,44].

Table 3. Fitting parameters

Test sample	R_s (Ω)	Q_b	n_1	R_b $K.\Omega\text{cm}^2$	Q_p	n_2	R_p Ωcm^2	Q_{ads}	n_3	R_{ads} Ωcm^2
Ti	19.3	$1.\times 10^{-5}$	0.798	36.0	7.4×10^{-5}	0.65	106	$0.5.\times 10^{-4}$	0.699	19.73
AT	20.2	$2.\times 10^{-8}$	0.931	68.8	1.6×10^{-4}	0.96	108	0.6×10^{-7}	0.890	500
Ca-P/AT	25.3	2×10^{-5}	0.903	90.1	1.1×10^{-5}	1.00	108	0.8×10^{-7}	0.917	743

The calculated impedance parameters were presented in Table 3. It is remarkable that the values of R_b and R_p for the AT and Ca-P/AT surfaces, respectively, are large in comparison with Ti surface. Those high values indicated that the compactness and the high passivity of these surfaces. The thicknesses of outer layer (Q_p ; taken as $1/C_p$) is of AT is larger than Ca-P/AT because it means that this film is capable of incorporating foreign ions like Ca^{+2} and PO_4^{-3} from ambient solution [40].

It is important to mention that the thickness of the BSA adsorption layer increase on both the AT and biomimetic Ca-P coating samples. The decrease of C_{ads} is due to the adsorption–desorption reactions occurring at the interface. The biomimetic Ca-P coating layer facilitates the adsorption of BSA [15]. It is also clear that increasing the value of R_{ads} for AT and Ca-P/AT surfaces, suggesting that good adhesion between albumin and such surfaces [24].

4. CONCLUSIONS

This work first described formation of biomimetic Ca-P coating formation on nano-porous AT film under simulated physiological solution. The results reveal that nano-porous TiO_2 surface is a good bioactive surface. The oxide film of Ti is formed exhibited excellent ability of inducing amorphous Ca-P coatings by immersing in SCPS for an hour at low temperature. The EIS measurements proved that the anodization treatment is not only just for surface passivating but also for bioactive treatment. Moreover, the AT and biomimetic Ca-P/AT surfaces increase the BSA adsorption.

ACKNOWLEDGEMENTS

The authors wish to acknowledge the King Fahed University of Petroleum and Minerals for financial support under (CR-12-2010).

References

1. M. B. Nasab, M. R. Hassan, *Trends Biomater. Artif. Organs*, 24 (1) (2010) 69.
2. Q.Mohsen, S.A.Fadl-Allah, *Mater. Corros.* 61(2010) 9999.
3. S.A.Fadl-Allah, Q.Mohsen, *Appl.Surf.Sci.* 256 (2010) 5849.

4. F.liu, F. wang, T.shimizu, K. Igarashi, I. Zhao, *Surf. Coat. Tech.* 199 (2005) 220
5. P. Habibovic, F. Barrere, K. de. Groot, in: R. L. Reis, S. Weiner (EdS.), *Learning from nature How to Design New Implantable Biomaterials*, Kluwer, *Dordrecht*, (2003) pp. 105
6. A.K. Shula, R. Balasubramaniam, S. Bhargava, *Journal of Alloys and Comp.*, 389 (1-2) (2005) 144.
7. J. Wang, P. Layrolle, M. Stigter, *Biomaterials*, 25 (2004) 583.
8. A.Bigia, E.Boaninia, B.Braccia, A.Facchinib, S.Panzavoltaa, F.Segattib, L.Sturbaa, *Biomaterials*, 26 (2005) 4085.
9. K. de Groot, J. G. C. Wolke, J. A. Jansen, *Proc. Inst. Mech. Eng.* 212 (1998) 137.
10. L.Sun, C.C.Berndt, K.A.crass, A.Kucuk, J.Biomed.Mater.Res.Appl.Biomater.58 (2001) 570.
11. M. F. Hsieh, L.-H. Perng, T.-S chin, *Mater. chem. phys.* 74 (2002) 245.
12. Y. Z. Yang, K. H. Kim, J. L. Ong, *Biomaterials*, 26 (2005) 327.
13. Q. Bao, C. Chem, D.wang, Q.Ji, T.lei, *Appl. Surf. Sci.*, 252 (2005) 1538.
14. H.B.Hu, C.J.lin, R.HU, Y.Leng, *Mater.Sci.Eng.*, 20 (2002) 209.
15. X, Lu, Z, Zhao, Y. leng; *Mater. Sci. Eng. C27* (2007) 700.
16. A. L. Yerokhin, X. Nie, A. Ley Land, A. Matthews, *Surf.Coat.Tech.* 130 (2000) 195.
17. S.V.Gnedenkov, O.A.Khrisanfova, A.G.zavidnaya, S.L.Sinbrukhov, P.S.Gordienko, S.I watsubo, A.Matsui, *Surf.Coat.Tech.* 145 (2001)146.
18. T.KoKubo, H.Kim, M.kawashita, *Biomaterials* 24 (2003) 2161.
19. P.Habibovic, F.Barrere, C.A.Van Blitterswik, K.de Groot, *Bone, Am.Cream.Soc.* 85 (2002) 517.
20. B.C.Yang, M.uchida, H.M.Kim, X.D.Zhang, T.KoKubo, *Biomaterials* , 25 (2004) 1003
21. W.H.Song, y.k.jun, Y.Han, S.H.Hong, *Biomaterials*, 25 (2004) 3341.
22. B.liang, S.Fujibayashi, M.Neo, J.tamura, H.K.Kim, M.Ucida, T.KoKubo, T.Nakamura, *Biomaterials*, 24 (2003) 4959.
23. D. G. Castner, B. D. Ratner, *Surf. Sci.* 500 (2002) 28.
24. N.P.Cosman, K.Fatih, S.G.Roscoe, *J.Electro.Analy*, 261 (2005) 574.
25. T. Byrne, L. Lohstreter, M. J. Filiaggi, Zhijun Bai, J. R. Dahn, *Surf. Sci.* 602 (2008) 2927.
26. J.M.Anderson, *Annual Review of Materials Research*, 31(2001) 81.
27. H.Elwing, *Biomaterials*, 19 (1998) 397.
28. R.T.T.Gettens, Z.J.Bai, J.L.Gilbert, *J.Biomedical.Materials.Research*, 72 (2005) 246.
29. E.Blomberg, P.M.Claesson, j.C.Froberg, *Biomaterials*, 19 (1998)1371.
30. E.A.Sprague, J.C.Palmaz, *Journal of Endovascular therapy*, 12 (2005) 594.
31. S.A. Fadl-Allah, R.M. El-Sherief, W.A. Badawy, *J Appl. Electrochem.* 38 (2008) 1459.
32. B.B.Lakshmi, C.J.Patrissi, C.R.Martin, *Chem.Mater.* 9 (1997) 2544.
33. Z.Miao, D.Xu, J.Ouyang, G.Guo, X.Zhao, Y.Tang, *Nano Lett.* 2 (2002)717.
34. A.Kar, K.S.Raja, M.Misra, *Surf.Coat.Technol.* 201 (2006) 3723.
35. R.Narayanan, H-J Lee, T-Y Kwon, K-H Kim, *Mater. Chemistry and Physics*, 125 (2011) 510.
36. S.Omanovic, S.G.Roscoe, *J.Colloid Interf.Sci.* 227 (2000) 2452.
37. A. Misheard, C. Aparicio, B.D. Ratner, J.A. Planell, J.Gil, *Biomaterials* 28 (2007) 586.
38. H.Tsuchiya, J.M.Macak, L.Muller, P.Greil, S.Virtanen, P.Schmuki, *J.Biomed.Mater.Res.* 77A (2006) 2544.
39. S.Oh, S.Jin, *Mater.Sci.Eng.* 26 (2006)1301.
40. R.Narayanan, H.J.lee, T.Y.Kwon, K.H.Kim, *Mater.Chem. & Phys.* 125 (2011) 510.
41. J.R. Macdonald, *Impedance Spectroscopy*, Wiley, New York, 1987.
42. J.Pan, D.Thierry, C.Leygraf, *Electrochim.Acta*, 41(1996) 1143.
43. W.A. Badawy, A. M. Fathi, R. M. El-Sherief, S. A. Fadl-Allah, *J.Alloy.Comp.* 47 (2009) 911.
44. G.Rondelli, P.Toricelli, M.Fini, R.Giardino, *Biomaterials*, 26 (2005) 2739.